

COMPARISON OF VERTICAL LAND MOTION SOLUTIONS IN THE CHESAPEAKE BAY

Madeline Kronebusch¹, D. Sarah Stamps¹

¹Virginia Tech Department of Geosciences

1. Abstract

Accurate estimates of vertical land motion (VLM) are critical for projecting relative sea level rise along coastlines. The Chesapeake Bay region is a hotspot of negative VLM (subsidence) on the U.S. East Coast. In collaboration with a consortium led by the USGS, a new VLM solution was derived for the Chesapeake Bay region using more than 55 campaign Global Positioning System (GPS) observations. We utilize this campaign GPS-derived solution as a baseline for comparison with a recently published solution for the U.S. East Coast based on a combination of Interferometric Synthetic Aperture Radar (InSAR) and Global Navigation Satellite Systems (GNSS). VLM Differences between the combined InSAR and GNSS solution and the campaign GPS-derived VLM solution range from -3.95 mm/year to 7.30 mm/year, with an average discrepancy of 0.64 mm/year. Conventional statistical significance was not achieved when comparing the VLM difference with the GPS monument types or when comparing the VLM difference with associated National Land Cover Database (NLCD) values. This suggests that other factors, such as temporal resolution or local subsurface geology, may better explain VLM discrepancies.

2. Introduction

Relative Sea level rise (RSLR), driven by global climate change¹, can cause hazards for coastal communities, including increased flooding and aquifer saltwater intrusion². Low elevation coastal zones (<10 m above sea level) cover two percent of the global land area yet contain ten percent of the global population³ and U.S. coastal counties, excluding the Great Lakes, support 30 percent of the U.S. population⁴. Quantification of RSLR and associated coastal hazard threats helps inform resilience in these communities to changing coastal conditions. Elevated levels of RSLR outpacing marsh vertical accumulation also impact the biodiversity and stability of the coastal environment which can deteriorate coastal ecosystem services including the natural storm buffering system⁵⁻⁷.

VLM is a factor that contributes to RSLR and varies spatially across the U.S. East Coast with particularly high VLM subsidence in the Chesapeake Bay region⁸⁻⁹. Since VLM measurements have varied throughout the Chesapeake Bay region, and there are different conclusions on regional negative vertical land motion (subsidence) averages, from -1.93 mm/yr¹⁰ to -1.5 mm/yr^{11,12}, and measurements of subsidence exceeding 5mm/yr¹³, continued efforts to combine local-scale observations to constrain regional subsidence rates are underway. When VLM solutions are produced, there is a need to compare results across studies to assess agreement and further refine VLM estimates. Two recent studies of VLM^{13,14}, drawing from different observational sources, have potential for comparison and synthesis to produce a high-resolution assessment of the Chesapeake Bay region and increase confidence in measured subsidence rates for estimating RSLR rates and resulting impacts on coastal communities.

Integrating InSAR and GPS data is an increasingly valuable approach for monitoring VLM. The high spatio-temporal resolution of InSAR measurements provide increased VLM measurement capability in coastal regions that are difficult to access, such as wetlands¹⁵ can be especially valuable. It is important to recognize that the depth of installation for point measurements such as GNSS or GPS are aligned with measuring certain types of VLM that are depth-dependent¹⁶. For example, GPS stations with deep rod installation will record deep subsidence (possibly tectonic in origin) while shallow-surface GPS monuments will measure shallow subsidence (which can be primarily controlled by shallow sediment compaction that has high spatial variability over short distances)^{16,17}. As a result, studies have called for integration of multiple VLM measurement methods¹⁸, including GPS, GNSS, and InSAR into regional estimates of RSLR¹⁹. Quantifying variability in VLM measurements between GPS-derived VLM solutions and InSAR-derived VLM solutions in the Chesapeake Bay will further ability to combine understanding multiple observation platforms in VLM campaigns.

3. Data

3.1 GPS-derived VLM solution

An annual observational campaign funded by the U.S. Geological Survey (USGS) spanning five years from 2019-2023 collected millimeter-precision VLM measurements (Figure 1) using GPS receiver stations installed and in operation for two weeks each October¹⁴. The 2019²⁰, 2020²¹, 2021²², 2022²³, and 2023²⁴ datasets are made publicly available through EarthScope Consortium for data preservation and management. GAMIT-GLOBK and OPUS Projects will produce two independent velocity solutions from the Chesapeake Bay GPS campaign data. The separation of the long-term VLM signals from the short-term VLM signals seeks to provide greater understanding of VLM drivers in the Chesapeake Bay region¹⁴.

3.2 Combined InSAR-GNSS VLM solution

A recently published study¹³ of VLM over the U.S. East Coast has generated a velocity solution (Figure 2) using GNSS and SAR data that can be compared to that of the USGS funded campaign¹³. The GNSS data from 2007-2020 is made available by the Nevada Geodetic Lab [<http://geodesy.unr.edu>]. The SAR datasets come from two different satellites: Sentinel-1A/B from 2015-2020 and ALOS from 2007-2011¹³. The combined SAR is transformed into a 3D line of sight (LOS) velocity using the wavelet based InSAR (WabInSAR)^{25,26} algorithm and after using a unified weighted least-squares joint optimization model, the 3D deformation field at each pixel was determined. The project enabled interpolation of VLM velocities over the national land cover pixels to determine VLM by land cover¹³.

3.3 NLCD Data

The 2019 National Land Cover Database (NLCD)²⁷, a standardized and nationwide dataset developed by the Multi-Resolution Land Characteristics (MRLC) Consortium, was used in comparisons. The NLCD provides 30-meter resolution land cover classifications derived primarily from Landsat 8 Operational Land Imager (OLI) imagery, enabling detailed analysis of land surface

properties across the United States. The majority land cover class within a 500-meter radius around each USGS campaign GPS station was extracted and used to assess the influence of surrounding land cover on vertical land motion differences. The NLCD categories were further grouped into broader land cover types (e.g., Water, Vegetated, Developed) to facilitate statistical analysis.

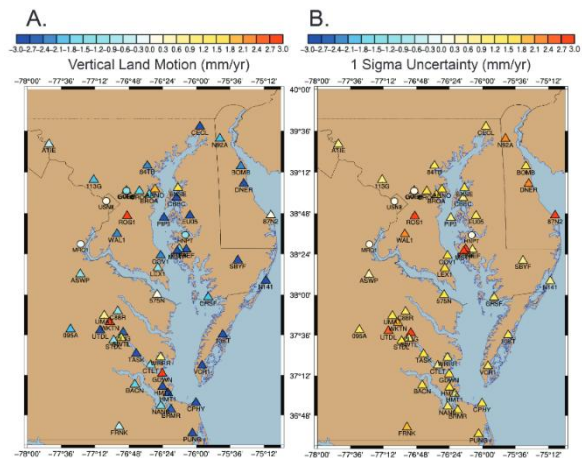
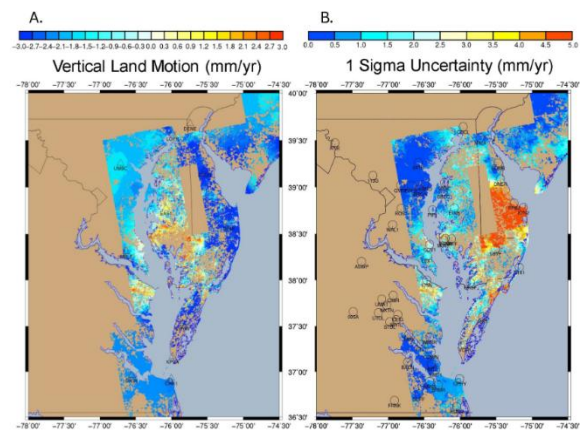


Figure 1. A. GPS-Derived VLM solution based on the USGS campaign data mapped in a color scale ranging from -3.0 mm/yr to 3.0 mm/yr. B.



Associated 1 sigma uncertainties. Figure 2. A. InSAR-derived VLM solution mapped in a color scale ranging from -3.0 mm/yr to 3.0 mm/yr with GNSS stations plotted as triangles. B. Associated 1 sigma uncertainties with locations of the USGS GPS benchmark as circles.

4. Methods

VLM estimates were compared from the GPS-derived VLM solution and the Combined InSAR-GNSS VLM solution within the Chesapeake Bay region, focusing on evaluating discrepancies across GPS monumentation types and land cover classes to understand potential spatial biases VLM Difference calculations.

4.1 Data Preparation and Spatial Alignment

The GPS-derived VLM solution and the Combined InSAR-GNSS VLM solution locations in decimal degrees were rounded to 3 decimal places and 2 decimal places respectively. The distance between each data point in the INSAR dataset and the GPS dataset is found using the “Haversine” Function (calculates the distance between two points on the Earth’s Surface which is a geodesic measurement). All INSAR-based VLM values located within 500 meters of the GPS station were averaged to compare with the corresponding GPS station VLM measurement.

4.2 Discrepancy Calculation

The difference between InSAR and GPS VLM was calculated at each station:

$$VLM\ Difference = InSARVLM_{avg} - GPSVLM \quad (1)$$

Where $InSARVLM_{avg}$ is the InSAR-based VLM averaged within 500 meters of the GPS station and $GPSVLM$ is the GPS-derived VLM solution at the corresponding GPS station. This VLM Difference value was then stored for later statistical and geospatial analyses.

4.3 Land Cover Classification and Analysis

Each GPS station was assigned a land cover class using the 2019 National Land Cover Database (NLCD). A 500-meter radius buffer was computed surrounding the GPS site. Then, the majority raster value within that buffer of the 2019 NLCD dataset was computed.

To assess whether InSAR-GPS VLM discrepancies differ significantly across land

cover classes, a one-way Analysis of Variance (ANOVA) test was performed on three classes: Water, Vegetated, and Developed. Each GPS station was assigned to one of these classes based on the majority NLCD 2019 land cover value within a 500-meter radius. The Water category included NLCD classes 11 and 12, Vegetated included classes 31, 41–43, 52, 71, 81, 82, 90, and 95, and Developed included classes 21–24. ANOVA tests the null hypothesis that all groups (land cover types) have equal mean discrepancies (Field, 2013).

4.4 Geodetic Monument Analysis

In addition to land cover classification, the type of GPS monumentation used at GPS sites was compared to the VLM Differences. Monument types across the Chesapeake Bay GPS campaign stations include deep rod monuments, surface monuments, disks on short rods, and massive concrete structures, each with differing degrees of structural coupling to the underlying Earth. These various monumentation types measure different types of motion and therefore result in different VLM measurements.

To assess this, each GPS station was labeled with its monumentation class based on metadata from the USGS campaign records. The VLM Difference at each site was then grouped by monument type to assess whether certain installation types were more prone to measurement inconsistency.

Each GPS station was classified as either a Surface or Deep Rod monument based on its construction type. The Surface category included stations mounted at or near the ground surface, such as those on buildings or shallow foundations. The Deep Rod category included stations anchored deeper into the ground, such as those installed using steel rods or other intermediate anchoring methods. These categories were used to examine whether monument construction influences the discrepancies between GPS- and InSAR-derived VLM estimates. A two-sample independent t-test was performed to evaluate whether the absolute vertical land motion (VLM) differences between GPS- and InSAR-derived estimates varied significantly by GPS monument type.

5. Results

Calculation of VLM Differences produced a summary map across the Chesapeake Bay region at USGS campaign GPS sites (Figure 3). VLM Differences between the combined InSAR and GNSS solution and the campaign GPS-derived VLM solution range from -3.95 mm/year to 7.30 mm/year, with an average discrepancy of 0.64 mm/year.

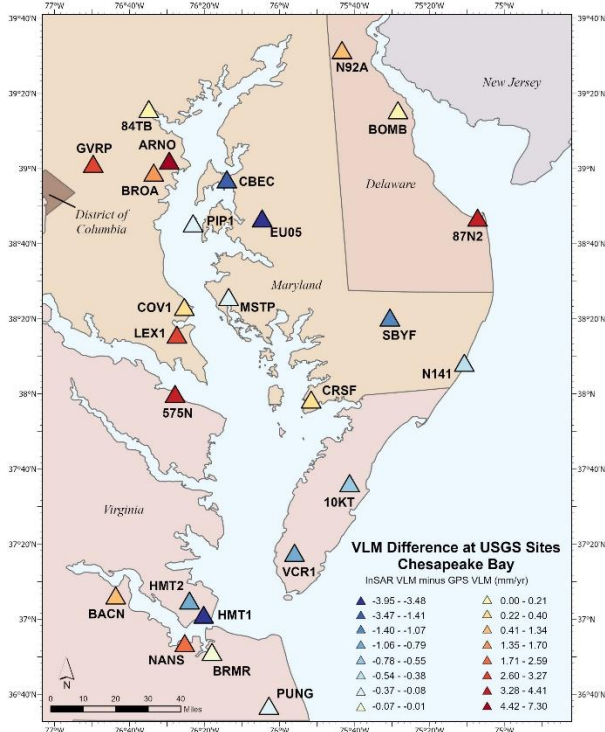


Figure 3. Plot of discrepancies where there are VLM solutions.

There was poor correlation between GPS VLM and InSAR VLM and the VLM Differences were skewed right (Figure 4).

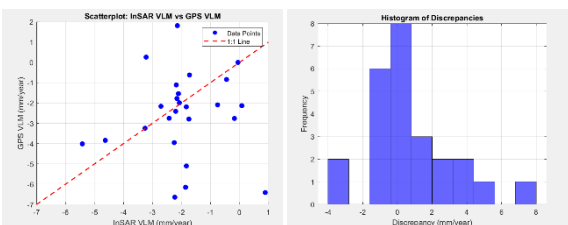


Figure 4. Left. Scatterplot of InSAR-based VLM and GPS-derived VLM. Right. Histogram of discrepancies.

After conducting the two-sample t-test to assess whether the absolute vertical land motion (VLM) discrepancies between GPS and InSAR differed by GPS monument type. The mean absolute VLM difference was 2.52 mm/yr (SD = 2.24, $n = 11$) for Surface monuments and 1.08 mm/yr (SD = 1.13, $n = 14$) for Deep Rod monuments. Although Surface monuments exhibited larger discrepancies on average, the difference was not statistically significant, t -statistic = 1.939, $p = 0.073$. This suggests a potential trend toward greater inconsistency in Surface monuments, but the result does not meet the standard threshold for statistical significance ($p < 0.05$).

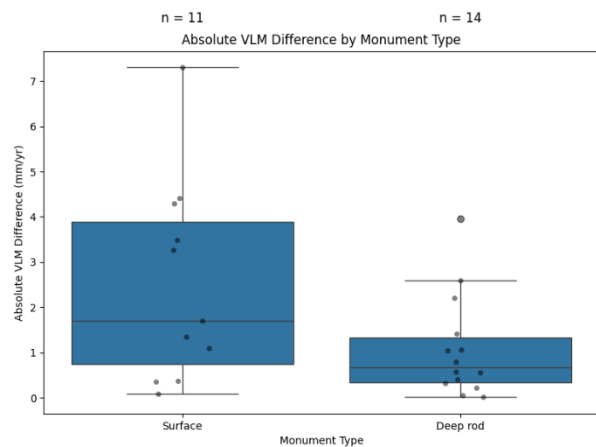


Figure 5. Boxplot showing the absolute vertical land motion (VLM) difference between GPS-derived and Combined InSAR-GNSS measurements by monument type.

A one-way Analysis of Variance (ANOVA) was performed to examine whether the absolute vertical land motion (VLM) differences between GPS and InSAR measurements varied by surrounding land cover type. The average absolute VLM discrepancy was highest in Developed areas (Mean = 2.19 mm/yr, SD = 2.25, $n = 10$), followed by Water (Mean = 1.90 mm/yr, SD = 1.89, $n = 5$), and Vegetated areas (Mean = 1.14 mm/yr, SD = 1.25, $n = 10$).

However, the ANOVA revealed that these differences were not statistically significant, $F\text{-statistic} = 0.85$, $p = 0.441$, suggesting that land cover type was not a major driver of GPS–InSAR VLM discrepancies in this dataset.

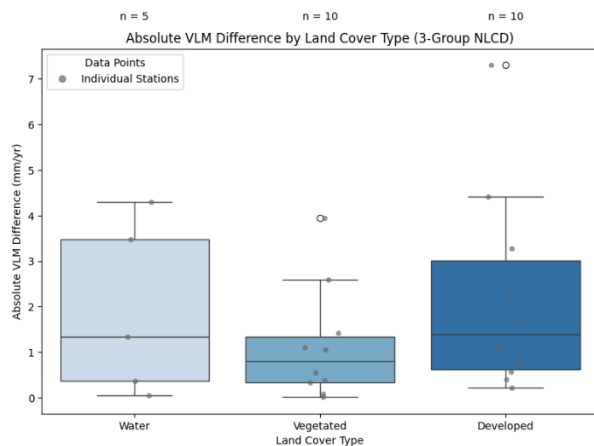


Figure 6. Boxplot showing the absolute vertical land motion (VLM) difference between GPS and InSAR measurements, grouped by generalized NLCD 2019 land cover class.

7. Conclusion

This study compared vertical land motion (VLM) estimates derived from campaign GPS observations and a combined InSAR-GNSS solution across the Chesapeake Bay region. By examining discrepancies between these two datasets, we assessed the influence of GPS monumentation type and surrounding land cover class on measurement differences. VLM discrepancies ranged from -3.95 mm/year to 7.30 mm/year, with an average difference of 0.64 mm/year. Although Surface-mounted GPS stations exhibited larger VLM discrepancies compared to Deep Rod installations, the difference was not statistically significant. These results would likely be improved using a larger sample size of GPS station locations. Similarly, no significant differences in VLM discrepancies were found across major land cover types, including Developed, Vegetated, and Water classes. These results suggest that neither monumentation type nor land cover alone fully explain the observed VLM differences between the two datasets. Instead, the discrepancies may reflect a combination of

factors, including the vertical sensitivity of InSAR, differences in temporal resolution, and local geologic or hydrologic conditions. Continued integration of geodetic datasets and exploration of additional environmental variables will be key to refining future VLM estimates that support coastal resilience planning.

8. Acknowledgements

Thank you to the VSGC Undergraduate STEM Research Scholarship Program for funding my work and to my project supervisor Dr. Stamps for her support and guidance. Thank you also to everyone in the VT Geodesy and Tectonophysics Laboratory, especially Karen Williams, for their feedback, and to the VT Geosciences Department for logistical support. Special thanks to Dr. Philippe Hensel, Dr. William Moore, and Ryan Hippenstiel for their contributions to project development and advice.

Literature Cited

- Allison, M. et al. Global Risks and Research Priorities for Coastal Subsidence. *Eos (Washington DC)* 97, (2016).
- Hauer, M. E. et al. Sea-level rise and human migration. *Nature Reviews Earth and Environment* vol. 1 Preprint at <https://doi.org/10.1038/s43017-019-0002-9> (2020).
- McGranahan, G., Balk, D. & Anderson, B. The rising tide: Assessing the risks of climate change and human settlements in low elevation coastal zones. *Environ Urban* 19, (2007).
- Crowell, M., Edelman, S., Coulton, K. & McAfee, S. How many people live in coastal areas? *Journal of Coastal Research* vol. 23 Preprint at <https://doi.org/10.2112/07A-0017.1> (2007).
- Blankespoor, B., Dasgupta, S. & Laplante, B. Sea-Level Rise and Coastal Wetlands. *Ambio* 43, (2014).
- Schuerch, M. et al. Future response of global coastal wetlands to sea-level rise. *Nature* 561, (2018).

7. Kirwan, M. L. & Megonigal, J. P. Tidal wetland stability in the face of human impacts and sea-level rise. *Nature* vol. 504 Preprint at <https://doi.org/10.1038/nature12856> (2013).
8. Sallenger, A. H., Doran, K. S. & Howd, P. A. Hotspot of accelerated sea-level rise on the Atlantic coast of North America. *Nat Clim Chang* 2, (2012).
9. Eggleston, J. & Pope, J. Land Subsidence and Relative Sea-Level Rise in the Southern Chesapeake Bay Region. USGS Circular 1392 (2013).
10. Peltier, W. R., Argus, D. F. & Drummond, R. Space geodesy constrains ice age terminal deglaciation; the global ICE-6G_C (VM5a) model. *J Geophys Res Solid Earth* 120, 450–487 (2015).
11. Sella, G. F. et al. Observation of glacial isostatic adjustment in ‘stable’ North America with GPS. *Geophys Res Lett* 34, (2007).
12. Kreemer, C., Hammond, W. C. & Blewitt, G. A Robust Estimation of the 3-D Intraplate Deformation of the North American Plate From GPS. *J Geophys Res Solid Earth* 123, (2018).
13. Ohenhen, L. O., Shirzaei, M., Ojha, C. & Kirwan, M. L. Hidden vulnerability of US Atlantic coast to sea-level rise due to vertical land motion. *Nat Commun* 14, (2023).
14. Troia, G. et al. GPS data from 2019 and 2020 campaigns in the Chesapeake Bay region towards quantifying vertical land motions. *Sci Data* 9, (2022).
15. Oliver-Cabrera, T., & Wdowinski, S. (2016). InSAR-Based Mapping of Tidal Inundation Extent and Amplitude in Louisiana Coastal Wetlands. *Remote Sensing (Basel, Switzerland)*, 8(5), 393–393. <https://doi.org/10.3390/rs8050393>
16. Langbein, J., & Svarc, J. L. (2019). Evaluation of Temporally Correlated Noise in Global Navigation Satellite System Time Series: Geodetic Monument Performance. *Journal of Geophysical Research. Solid Earth*, 124(1), 925–942. <https://doi.org/10.1029/2018JB016783>
17. Jankowski, K. L., Törnqvist, T. E., & Fernandes, A. M. (2017). Vulnerability of Louisiana’s coastal wetlands to present-day rates of relative sea-level rise. *Nature Communications*, 8(1), 14792–14792. <https://doi.org/10.1038/ncomms14792>
18. Cahoon, D. R. (2015). Estimating Relative Sea-Level Rise and Submergence Potential at a Coastal Wetland. *Estuaries and Coasts*, 38(3), 1077–1084. <https://doi.org/10.1007/s12237-014-9872-8>
19. Keogh, M. E., & Tornqvist, T. E. (2019). Measuring rates of present-day relative sea-level rise in low-elevation coastal zones: a critical evaluation. *Ocean Science*, 15(1), 61–73. <https://doi.org/10.5194/os-15-61-2019>
20. Troia, G. S. D. S. H. P. et al. , Chesapeake Bay Vertical Land Motions 2019. GPS/GNSS Observations Dataset (2020). <https://doi.org/10.7283/M6D3-T837>
21. Gabrielle Troia, D. S. S. P. H. et al. , Chesapeake Bay Vertical Land Motions 2020. GPS/GNSS Observations Dataset (2022). <https://doi.org/10.7283/98DG-AJ14>
22. Madeline Kronebusch, G. T. D. S. S. et. al.,. Chesapeake Bay Vertical Land Motions 2021. GPS/GNSS Observations Dataset (2022). <https://doi.org/10.7283/4ENN-6906>
23. Anabelle Fry, M. K. H. H. et al. , Chesapeake Bay Vertical Land Motions 2022. GPS/GNSS Observations Dataset (2023). <https://doi.org/10.7283/6BKC-4A59>
24. Williams, Karen, et al., Chesapeake Bay Vertical Land Motions 2023, NSF GAGE Facility, GPS/GNSS Observations Dataset (2024) <https://doi.org/10.7283/2BBS-GE19>
25. Shirzaei, M. & Bürgmann, R. Topography correlated atmospheric delay correction in radar interferometry using wavelet transforms. *Geophys Res Lett* 39, (2012).
26. Shirzaei, M. A wavelet-based multitemporal DInSAR algorithm for

monitoring ground surface motion. IEEE
Geoscience and Remote Sensing Letters 10,
(2013).

27. Dewitz, J., 2021, *National Land Cover
Database (NLCD) 2019 Land Cover Science
Product (ver. 2.0, June 2021)*: U.S.
Geological Survey data release,
<https://doi.org/10.5066/P9KZCM54>.